Proc. Int. Symp. for Ultra-High Energy Cosmic Rays (UHECR2014)
JPS Conf. Proc. **9**, 010010 (2016)
http://doi.org/10.7566/JPSCP.9.010010

KASCADE-Grande
Review, Recent Results, Future Endeavors

S. Schoo[1], W.D. Apel[1], J.C. Arteaga-Velázquez[2], K. Beck[1], M. Bertaina[3], J. Blümer[1,4], H. Bozdog[1], I.M. Brancus[5], E. Cantoni[3,6,a], A. Chiavassa[3], F. Cossavella[4,b], K. Daumiller[1], V. de Souza[7], F. Di Pierro[3], P. Doll[1], R. Engel[1], D. Fuhrmann[8,c], A. Gherghel-Lascu[5], H.J. Gils[1], R. Glasstetter[8], C. Grupen[9], A. Haungs[1], D. Heck[1], J.R. Hörandel[10], D. Huber[4], T. Huege[1], K.-H. Kampert[8], D. Kang[4], H.O. Klages[1], K. Link[4], P. Łuczak[11], H.J. Mathes[1], H.J. Mayer[1], J. Milke[1], B. Mitrica[5], C. Morello[6], J. Oehlschläger[1], S. Ostapchenko[12], N. Palmieri[4], M. Petcu[5], T. Pierog[1], H. Rebel[1], M. Roth[1], H. Schieler[1], F.G. Schröder[1], O. Sima[13], G. Toma[5], G.C. Trinchero[6], H. Ulrich[1], A. Weindl[1], J. Wochele[1], J. Zabierowski[11]

[1]*Institut für Kernphysik, KIT - Karlsruhe Institute of Technology, Germany*
[2]*Universidad Michoacana de San Nicolas de Hidalgo, Inst. F´sica y Matemáticas, Morelia, Mexico*
[3]*Dipartimento di Fisica, Universitá degli Studi di Torino, Italy*
[4]*Institut für Experimentelle Kernphysik, KIT - Karlsruhe Institute of Technology, Germany*
[5]*Horia Hulubei National Institute of Physics and Nuclear Engineering, Bucharest, Romania*
[6]*Osservatorio Astrofisico di Torino, INAF Torino, Italy*
[7]*Universidade São Paulo, Instituto de F sica de São Carlos, Brasil*
[8]*Fachbereich Physik, Universität Wuppertal, Germany*
[9]*Department of Physics, Siegen University, Germany*
[10]*Dept. of Astrophysics, Radboud University Nijmegen, The Netherlands*
[11]*National Centre for Nuclear Research, Department of Astrophysics, Lodz, Poland*
[12]*Frankfurt Institute for Advanced Studies (FIAS), Frankfurt am Main, Germany*
[13]*Department of Physics, University of Bucharest, Bucharest, Romania*
[a]*now at: Istituto Nazionale di Ricerca Metrologia, INRIM, Torino*
[b]*now at: DLR Oberpfaffenhofen, Germany*
[c]*now at: University of Duisburg-Essen, Duisburg, Germany*

E-mail: sven.schoo@kit.edu

A detailed knowledge of the energy spectrum and composition of cosmic rays (CRs) is the most important source of information for solving the riddle of the origin of CRs. The KASCADE experiment and its extension KASCADE-Grande have contributed much to the current knowledge about both the spectrum and composition in the energy range from around 1 PeV to 1 EeV. One of the most important results of the KASCADE experiment is the connection of the knee at a few PeV to a decrease in the flux of light primaries. Later, KASCADE-Grande found a knee-like structure also in the spectrum of heavy elements at around 90 PeV and an ankle-like feature in the spectrum of light elements just above 100 PeV. In this contribution a short review of the experiment will be followed by an overview on the current results on spectrum and composition of CRs and a summary of the further activities within the KASCADE-Grande collaboration related to both, data analysis and data publication.

KEYWORDS: UHECR 2014, KASCADE, KASCADE-Grande, air shower experiment, knee

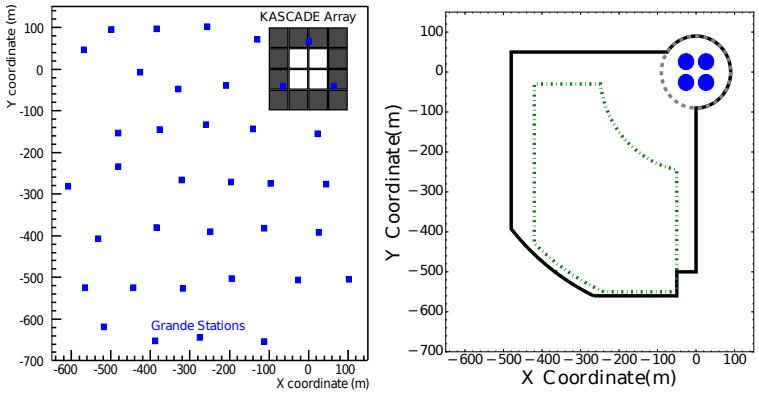

Fig. 1. Left: The Grande stations (blue rectangles) are shown together with the KASCADE-array. The grey shaded area corresponds to the outer 12 clusters (μ-detectors), the blank squares are the inner 4 clusters. Right: Selected fiducial areas used for the data analyses. The dashed circle corresponds to the area used for the standard KASCADE event selection. The other dashed lines depict the effective area used by most KASCADE-Grande analyses. The continuous lines and the four circles are used by the combined analysis (see section 2).

1. Summary of Recent Results

The KASCADE-array (Lon.: 8.4°, Lat.: 49.1°, Alt.: 110 m a.s.l) consisted of 252 detector stations organized in 16 clusters. The outer 12 clusters (gray shaded squares in Fig. 1) grouped 192 stations equipped with shielded and non-shielded scintillation detectors. This configuration made possible the separation of the number of muons (N_μ) from the total number of charged particles (N_{ch}). Taking into account the ratio of photons to electrons and their mean energy deposit (both inferred from simulations, see [5]) it was possible to derive the number of electrons at observation level (N_e). The inner four clusters (blank squares in Fig. 1) have been equipped with twice the number of non-shielded scintillation detectors, but did not include shielded detectors.

Both, N_e and N_μ are in principle sensitive to the energy of the primary particle, however, only the simultaneous usage of both observables takes the mass dependence into account. Therefore, the analysis of the KASCADE data [6] is based on the two-dimensional shower-size spectrum that is shown on the left hand side (l.h.s.) of Fig. 2. The contents of each cell may be expressed in the following way:

$$\vec{Y} = \mathbf{R}\vec{X} \tag{1}$$

with $\vec{Y}$ describing the reconstructed N_e and N_μ, $\vec{X}$ being the corresponding mass and energies of the primary particles and **R** being the *response matrix*. The latter takes into account the probabilities of a particle with a specified mass and energy inducing air-showers that, due to intrinsic shower-to-shower fluctuations, span distinct areas in the two-dimensional shower-size spectrum. This spectrum gets modified by trigger- and reconstruction probabilities for such showers and by inaccuracies in the reconstruction of N_e and N_μ. Based on the *response matrix*, an unfolding technique can be used to solve the inverse problem of inferring the energy spectra for particles of several individual mass groups. The results for proton, helium, and carbon primaries are shown on the right hand side (r.h.s.) of Fig. 2 using QGSJet01 [7] as the hadronic interaction model. The analysis included also spectra for silicon and iron compared also to the results for another hadronic interaction model, namely SIBYLL [8] (For details see [6]).

The knee in the all-particle spectrum at around 6 PeV was commonly expected to be due to a decrease of the flux of protons. However, the KASCADE results suggest that the knee might be dominated by a knee-like structure in the energy spectrum of helium, which seems, using QGSJet01

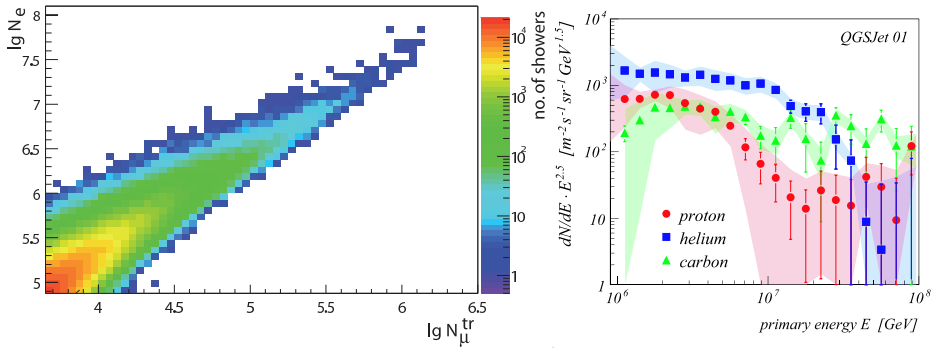

Fig. 2. Left: The two-dimensional shower-size spectrum measured with KASCADE.
Right: The resulting, unfolded spectra for proton and helium together with the all-particle spectrum (See [6]).

as the hadronic interaction model, to be more abundant than protons in that energy range. If this is true, the knee of e.g. iron - in the scenario of rigidity dependent knee-positions - would be expected to be around 100 PeV, which was the upper energy limit of the KASCADE-array and was one reason for building KASCADE-Grande.

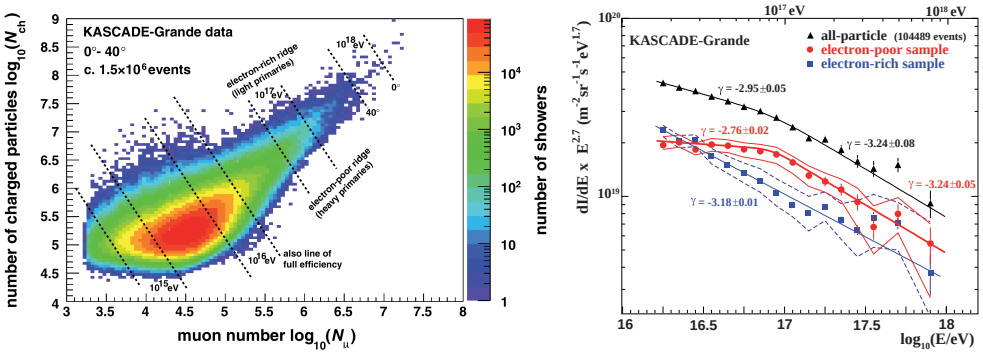

Fig. 3. Left: The two-dimensional shower size spectrum for KASCADE-Grande data.
Right: The energy spectra for all particles, light (electron-rich) and heavy (electron-poor) primaries based on the two-dimensional spectrum on the left side (See [10]).

KASCADE-Grande was located next to the KASCADE-array. The layout and the position of the scintillator-array relative to KASCADE is shown in Fig. 1. The 37 stations were equipped with non-shielded scintillation detectors only. Therefore, the shielded detectors of the KASCADE-array had to be used for the reconstruction of N_μ.

The reconstruction of the energy is based primarily on N_{ch} using the ratio of N_{ch} to N_μ as a function of N_{ch} to take into account the mass-dependence of the energy corresponding to a certain number of charged particles at ground. The two-dimensional shower-size spectrum for this analysis is shown on the l.h.s. of Fig. 3.

As explained in [9], the following formulas are used:

$$\log_{10}(E) = [a_H + (a_{Fe} - a_H) \cdot k] \cdot \log_{10}(N_{ch}) + b_H + (b_{Fe} - b_H) \cdot k \tag{2}$$

with

$$k = \frac{\log_{10}(N_{ch}/N_\mu) - \log_{10}(N_{ch}/N_\mu)_H}{\log_{10}(N_{ch}/N_\mu)_{Fe} - \log_{10}(N_{ch}/N_\mu)_H} \tag{3}$$

and

$$\log_{10}(N_{\mathrm{ch}}/N_{\mu})_{\mathrm{H,Fe}} = c_{\mathrm{H,Fe}} \cdot \log_{10}(N_{\mathrm{ch}}) + d_{\mathrm{H,Fe}} \tag{4}$$

The coefficients are derived using simulated showers for proton and iron primaries. The k parameter is mass sensitive, therefore, it can be used to separate the events in a light (electron-rich) and a heavy (electron-poor) mass group. This is done by comparing the measured value of k with the mean, energy-dependent values of k for simulations of showers induced by particles of five different masses. See [10, 11] for detailed descriptions of this procedure.

The results (using QGSJetII-02 [12]) are shown on the r.h.s. of Fig. 3. The all-particle spectrum shows a knee-like structure at an energy of about 80 PeV. The heavy component is defined by a separation between carbon and silicon. Its spectrum shows an even more prominent knee-like structure than in the all-particle spectrum at roughly the same energy. In combination with the KASCADE results shown in the last subsection, this is a strong indication for charge-dependent positions of the knee-like structures. At this point the exact composition of the heavy component is not known. In principle it could be dominated by e.g. silicon, therefore, the iron knee might be at a slightly higher energy. The role of the hadronic interaction model is also important in this context and will be discussed later.

Assuming the correctness of QGSJetII-02, the light component should not contain elements significantly heavier than carbon. There are hints for a recovery of the spectrum just above 100 PeV which was not found to be significant. However, the contribution of medium mass particles could mask an underlying feature in the spectra of lighter primaries.

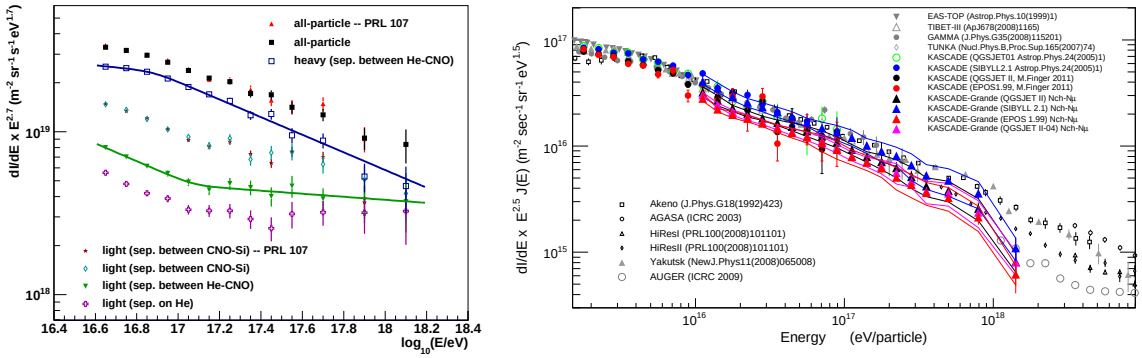

Fig. 4. Left: The energy spectra for all particles, light and heavy primaries for different separations [11]. Right: The all-particle energy spectra based on four different hadronic interaction models [14].

Another analysis aimed on investigating the spectral shape of the light CR component (dominated by the contribution of light primaries), trading a slightly higher energy threshold for a larger fiducial area (28 percent larger). The reconstruction strategy was the same as before. A comparison between the results of the analysis described in the last section and this one is shown on the l.h.s. of Fig. 4. The all-particle energy spectra of both analyses are in good agreement, the result for this analysis profiting slightly from the increased statistics from both, the larger fiducial area and a larger data-set including additional 87 days of data-taking. The heavy component shown here is defined a bit differently. Instead of using a separation between carbon and silicon, the separation is chosen to be between helium and carbon. Although there are only two or three sampling points for a fit below the knee-like structure, the existence of such a feature has been confirmed. As a cross-check the light component using the same separation as before is compared to the previous result being in good agreement with each other, which is another indication that both data-sets are compatible.

Now, with a possible influence of medium mass particles on the structures of the spectra of light primaries being reduced, the spectrum of the enhanced light component exhibits a significant recovery just above 100 PeV. In addition the slopes of the spectrum of heavy primaries above its knee-like feature and the slope of the spectrum of light primaries below the ankle-like feature are the same. This may indicate that both originate from the same astrophysical mechanism. If one assumes that the heavy component is the end of the galactic component, it would strongly suggest that the spectrum of light particles above the ankle-like feature is of extra-galactic origin. The composition of the light component depends on which elements contribute in that energy range and again on the hadronic interaction model.

A comparison of the all-particle spectra derived using four different models is shown on the r.h.s. of Fig. 4 [13, 14]. These results are again based on the method described above. A higher energy is assigned to the same measured event, if a model predicts less electrons and/or fewer muons compared to another model. If a model predicts fewer muons, the same event will seem to stem from a heavier particle. On the other hand, the more muons are predicted, the lighter the reconstructed composition becomes. For a certain measured number of charged particles, the reconstructed energy increases with the reconstructed mass of the primary particle. This is the reason why the flux reconstructed using EPOS based simulations, which predict more muons, is lower by about 10 percent compared to the one obtained using QGSJetII-02 based simulations. As is shown in [14], the ratio of N_{ch} to N_{μ} for SIBYLL is only slightly larger than the one for QGSJetII-02 simulations, therefore, the 25 percent larger flux is not caused by a smaller muon content, but predominantly by a smaller predicted number of electrons.

This has some implications regarding the influence of the hadronic interaction model on the reconstructed spectra for the separate mass groups (see Fig, 6). It is shown in [14,15], that for a EPOS based reconstruction the flux for the light component increases relative to the QGSJetII-02 results, while the flux of the heavy component decreases. The reconstructed energy at which the "heavy-knee" occurs decreases too, due to the lower mean energy that is assigned to the events. However, this shift (66 PeV instead of 83 PeV) is not large enough that one would exclude a possible charge dependent position of this feature, especially because the exact composition of the heavy component is not clear. Both, the lower mean energy and the larger light component result in an earlier crossing of the spectra of the heavy and light component.

Using SIBYLL results in quite the opposite. Due to the slightly larger ratio of N_{ch} to N_{μ}, one would expect a smaller light component, maybe something between the light components shown in Fig. 4 for the separation between carbon and helium and for the separation on helium. Indeed, the slope towards higher energies is less steep than the slope of the light component for QGSJetII-02. The flux, however, is larger, because of larger values for the mean reconstructed energy, which overcompensates the shift of measured events to the heavy mass group. The latter shows a knee-like structure that is shifted only slightly towards higher energies compared to QGSJetII-02 (91 PeV instead of 83 PeV).

An unfolding analysis like the one mentioned in the last section has also been performed for KASCADE-Grande data [16]. The results are shown in Fig. 5. The zenith angular range had been restricted to the interval from 0 to 18° (The standard range used for most analyses spans 0 to 40°). The respective decrease of the number of measured events impacted the analysis, especially at higher energies, where the number of events is already small to begin with. This is the main reason why this analysis stops at just above 100 PeV. For iron the systematic uncertainties are comparatively small and the knee-like structure observed in the analyses mentioned earlier is also visible here. For silicon the picture is not so clear. Due to the large systematic uncertainties a knee-like structure seems to be possible, but it is not immediately obvious. Interestingly, the proton spectrum hints at a possible recovery at around $10^{16.5}$ eV. There were hints on such a structure in the spectrum of the light component in other KASCADE-Grande based analyses. Unfortunately the spectra do not reach

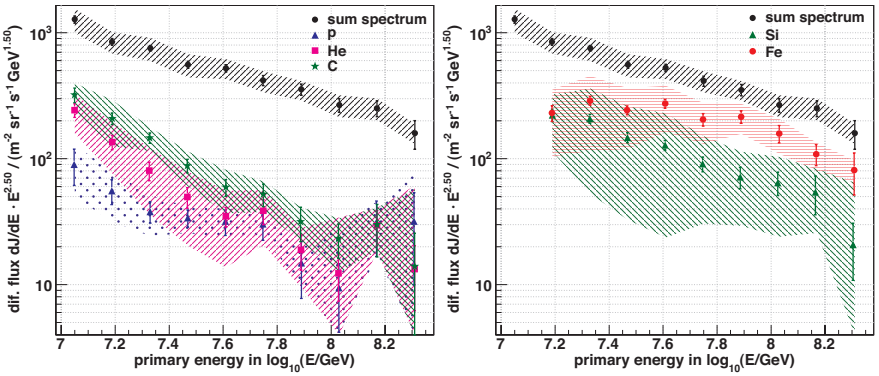

Fig. 5. The results of an unfolding analysis performed on KASCADE-Grande data ([16]).

far enough beyond 100 PeV to see how the proton and helium spectra evolve at higher energies and to get another hint at a possible composition around the ankle-like feature shown in Fig 4. It has to be stressed, that the complications based on the hadronic interaction models apply to this analysis, too.

Summarizing the results, a charge dependent connection of the knee-like structures in the spectra for individual masses and mass groups seems to be likely. However, due to the uncertainties in the composition it is not possible to exclude other scenarios. Possible scenarios that would result in charge dependent knee-positions include charge dependent acceleration mechanisms and the possibility of charge dependent leakage of CRs from our galaxy [17]. Both scenarios imply that beyond the proton knee, the contribution of light elements should become less important towards higher energies. This seems to be the case no matter which hadronic interaction model is used. More importantly the slopes of the spectra above the knee-like structures in the light and heavy components match, indicating that they may have the same astrophysical origin. If the charge dependence is indeed caused by a leakage of CRs from our galaxy, the incoming new component found in the spectrum of light elements could be of extragalactic origin. The most important result of the studies on the role of hadronic interaction models was that the existence of these features do not depend on the hadronic interaction model used. The interpretation might change, however, due to different abundances and slightly different energies at which the features occur.

2. Future Endeavors

Currently there are several analyses being performed. Using the KASCADE and KASCADE-Grande arrays, upper limits on the diffuse gamma ray flux are obtained [18]. Results for KASCADE-Grande are shown on the r.h.s. of Fig. 6. An update for KASCADE and a search for point-sources is also in the making.

Directly related to the problem of validity of the hadronic interaction models is an analysis that investigates the use of another observable, namely S500, for the reconstruction of the primary energy [19]. It is based on the assumption that, for the KASCADE-Grande array, the lateral density distributions for all elements cross at a distance of around 500 meters from the shower-core (Fig. 7, left plot). The density at this distance is, therefore, independent of the mass of the primary particle and its value is sensitive to the energy of the cosmic particle. This study includes a comparison to the other approaches.

An analysis that is currently in the process of being published, studies the attenuation of muons and charged particles in the Earth's atmosphere. This is especially interesting for cross-checking hadronic interaction models. It is based on the idea of constant-intensity that assumes a flux of CRs that is isotropic in zenith angle. The number of muons measured for a certain primary particle is de-

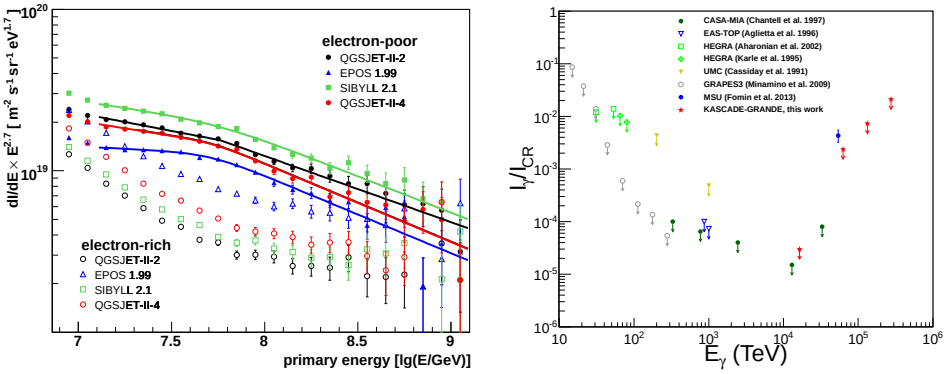

Fig. 6. Left: Energy spectra for light and heavy mass groups obtained using four different hadronic interaction models. (See [15]).
Right: Upper limits on the diffuse gamma ray flux relative to the measured CR flux (See [18]).

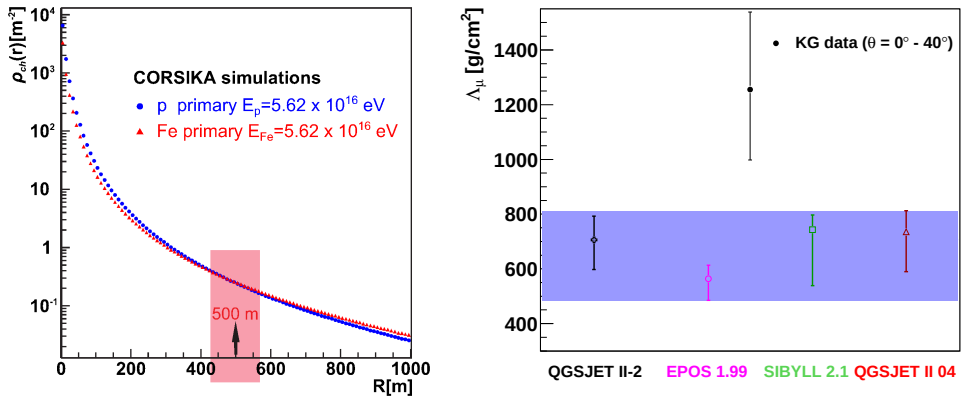

Fig. 7. Left: The lateral distributions for simulated proton and iron showers (See [19]).
Right: The muon attenuation length for measured data compared to simulations for four hadronic interaction models. (For both, see [20]).

creasing with increasing zenith angle, however, the same intensity corresponds to the same primary energy. Therefore, the shift in N_μ for the same cosmic ray intensity but different zenith angles corresponds to the attenuation of muons in the atmosphere. Some of the results are shown in Fig. 7. The errorbars are the combined systematic and statistical uncertainties. It is obvious that none of the four models correctly describes the observed attenuation length [20].

Another analysis aims at combining the KASCADE and KASCADE-Grande arrays right at the beginning of the reconstruction procedures. The number of charged particles and the number of muons is the result of a fit to the lateral densities measured by both detector setups. Therefore, events located in the Grande array gain additional 252 density measurements and events located in the KASCADE array gain 37 additional measurements and, more importantly, measurements at a larger distance to the shower core. This results in a higher accuracy of the reconstructed shower observables. In addition to that, a larger fiducial area can be selected as is shown in Fig. 1 as a solid line. It is by a factor of around 1.9 larger than the standard KASCADE-Grande area. The goal of this analysis is to obtain one, consistent energy spectrum for the combined energy-range from about 10^{15} to 10^{18} eV and possibly even down towards 10^{14} eV for events within a sub-KASCADE area selection (the four

circles shown in Fig. 1).

Last, but not least, the KASCADE-Grande Collaboration is developing a webportal that aims to provide easy and open access to reconstructed events that have been measured by the KASCADE-Grande experiment, including detailed information on the experiments' layout and example analyses meant to be an entry point for interested students. The project is called "KASCADE Cosmic Ray Data Centre" (KCDC) [21] and it currently provides 160 million events measured by the KASCADE-array and the hadron calorimeter. In total 18 observables are available for each event. These include environmental observables like the temperature and air pressure, information on measurement time, the core-position, arrival direction as well as information on the electron-, muon-, and hadron-content of the shower.

The number of events and the number of observables per event is going to increase during the next releases. For the future, the publication of KASCADE-Grande measurements and possibly of measurements from experiments that have been running alongside KASCADE-Grande, e.g. LOPES [22] and CROME [23] is planned. To make it easier for other experiments to publish their data, the software of KCDC will be made open-source in the future.

Acknowledgment

The authors would like to thank the members of the engineering and technical staff of the KASCADE-Grande collaboration, who contributed to the success of the experiment. The KASCADE-Grande experiment is supported in Germany by the BMBF and by the Helmholtz Alliance for Astroparticle Physics - HAP funded by the Initiative and Networking Fund of the Helmholtz Association, by the MIUR and INAF of Italy, the Polish Ministry of Science and Higher Education, and the Romanian Authority for Scientific Research UEFISCDI (PNII-IDEI grants 271/2011 and 17/2011).

References

[1] T. Antoni et al.: Nucl. Instrum. Methods Phys. Res., Sect. A **513** (2003) 490.
[2] W.D. Apel et al.: Nucl. Instrum. Methods Phys. Res., Sect. A **620** (2010) 202.
[3] W.D. Apel et al.: Astropart. Phys. **34** (2011) 476.
[4] W.D. Apel et al.: Astropart. Phys. **65** (2015) 55.
[5] W.D. Apel et al.: Astropart. Phys. **24** (2006) 467.
[6] T. Antoni et al.: Astropart. Phys. **24** (2005) 1.
[7] Kalmykov N.N., Ostapchenko S.S. and Pavlov A.I.: Nucl. Phys. B (Proc. Suppl.) **52** (1997) 17.
[8] Engel, R.: International Cosmic Ray Conference (1999).
[9] W.D. Apel et al.: Astropart. Phys. **36** (2012) 183.
[10] W.D. Apel et al.: Phys. Rev. Lett. **107** (2011) 171104.
[11] W.D. Apel et al.: Phys. Rev. D **87** (2013) 081101(R).
[12] S. Ostapchenko: Nucl. Phys. B, Proc. Suppl. **151** (2006) 143.
[13] W.D. Apel et al.: Adv. Space Res. **53** (2014) 1456.
[14] M. Bertaina et al.: Nucl. Phys. B, Proc. Suppl. **256-257** (2014) 149.
[15] Kang, D. et al.: International Cosmic Ray Conference (2013).
[16] W.D. Apel et al.: Astropart. Phys. **47** (2013) 54.
[17] G. Giacinti et al.: arXiv:1502.01608 [astro-ph.HE] (2015).
[18] Kang, D. et al.: European Cosmic Ray Symposium (2014).
[19] Toma, G. et al.: International Cosmic Ray Conference (2013).
[20] Arteaga-Velázquez, J.C. et al.: ISVHECRI (2014).
[21] see https://kcdc.ikp.kit.edu (2015).
[22] Falcke, H. et al.: Nature **435** (2005) 313.
[23] Smida, R. et al.: Phys. Rev. Lett. **113** (2014) 221101.